Supplementary Materials for "Berry Curvature Engineering by Gating Two-Dimensional Antiferromagnets"

Shiqiao Du,[1] Peizhe Tang,[2*] Jiaheng Li,[1], Zuzhang Lin,[3], Yong Xu,[1,4,5†], Wenhui Duan,[1,3,4‡] Angel Rubio,[2,6,7§]
[1] *State Key Laboratory of Low-Dimensional Quantum Physics, Department of Physics, Tsinghua University, Beijing 100084, China,*
[2] *Max Planck Institute for the Structure and Dynamics of Matter, Center for Free-Electron Laser Science, Luruper Chaussee 149, 22761 Hamburg, Germany.*
[3] *Institute for Advanced Study, Tsinghua University, Beijing 100084, China*
[4] *Collaborative Innovation Center of Quantum Matter, Beijing 100084, China*
[5] *RIKEN Center for Emergent Matter Science (CEMS), Wako, Saitama 351-0198, Japan*
[6] *Nano-Bio Spectroscopy Group, Departamento de Fisica de Materiales, Universidad del País Vasco UPV/EHU, 20018 San Sebastián, Spain. and*
[7] *Center for Computational Quantum Physics,Flatiron Institute, 162 Fifth Avenue, New York, NY 10010, USA.*
(Dated: April 7, 2020)

* Email: peizhe.tang@mpsd.mpg.de
† Email: yongxu@mail.tsinghua.edu.cn.
‡ Email: dwh@phys.tsinghua.edu.cn.
§ Email: angel.rubio@mpsd.mpg.de.

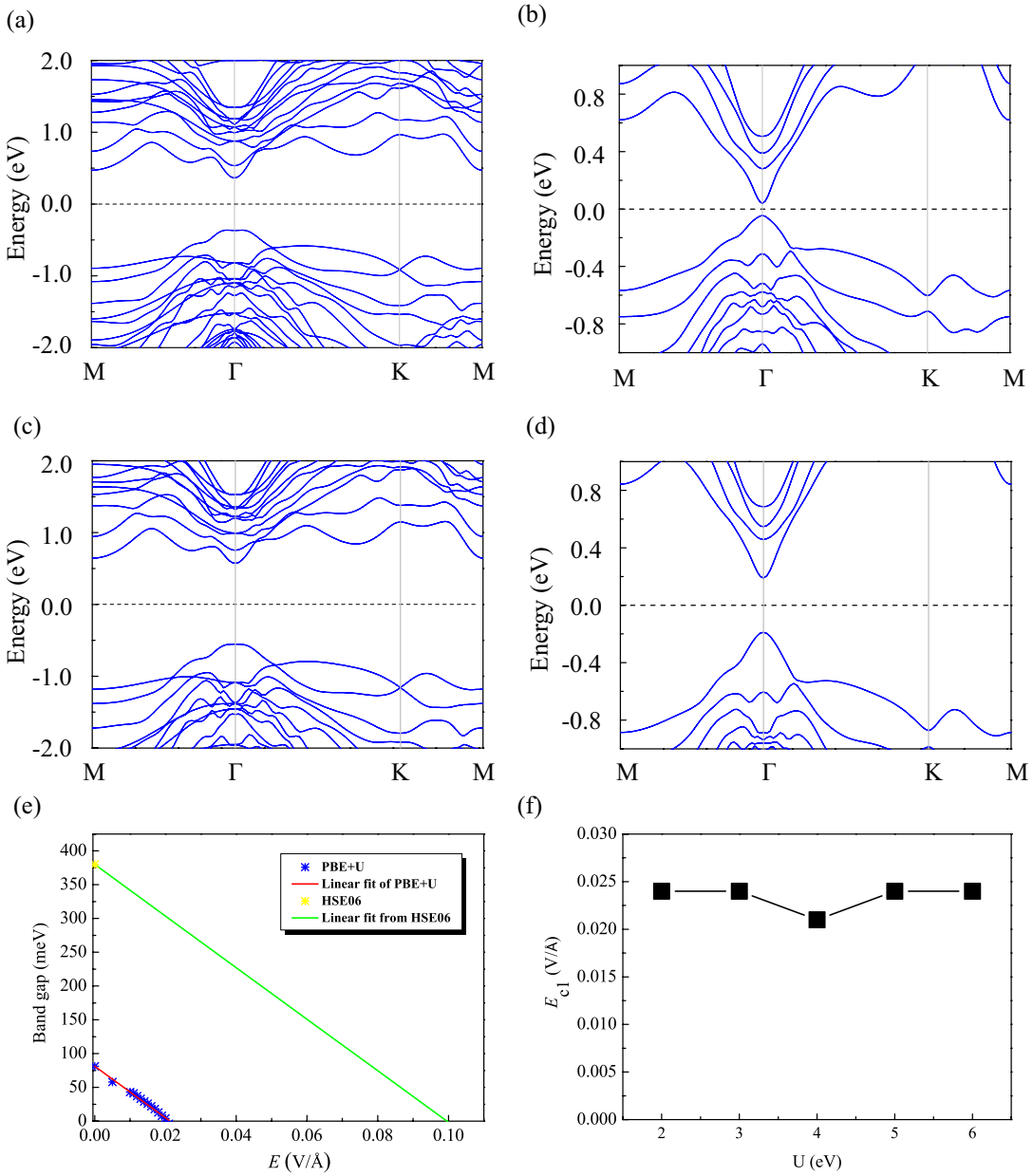

FIG. S1: Intrinsic band structures of double-SL $MnBi_2Te_4$ thin films using different exchange correlation functionals with and without SOC. (**A**) PBE+U without SOC; (**B**) PBE+U with SOC; (**C**) HSE06 without SOC; and (**D**) HSE06 with SOC. The Fermi level is set to zero and the band structures are doubly degenerated at each k point protected by the $\mathcal{PT}$ symmetry.(e) Band gaps of DFT calculations with different exchange-correlation functionals response to the change of electric fields. The blue stars represent the results by usingfrom PBE+U functional and the red line is the linear fit of that. The yellow star represents the result by using HSE06 functional and the green line is a linear function share the same slope with red line cross the yellow star. (f) The critical field E_{c1} (V/Å) depends on the choice of Hubbard U in PBE+U calculations.

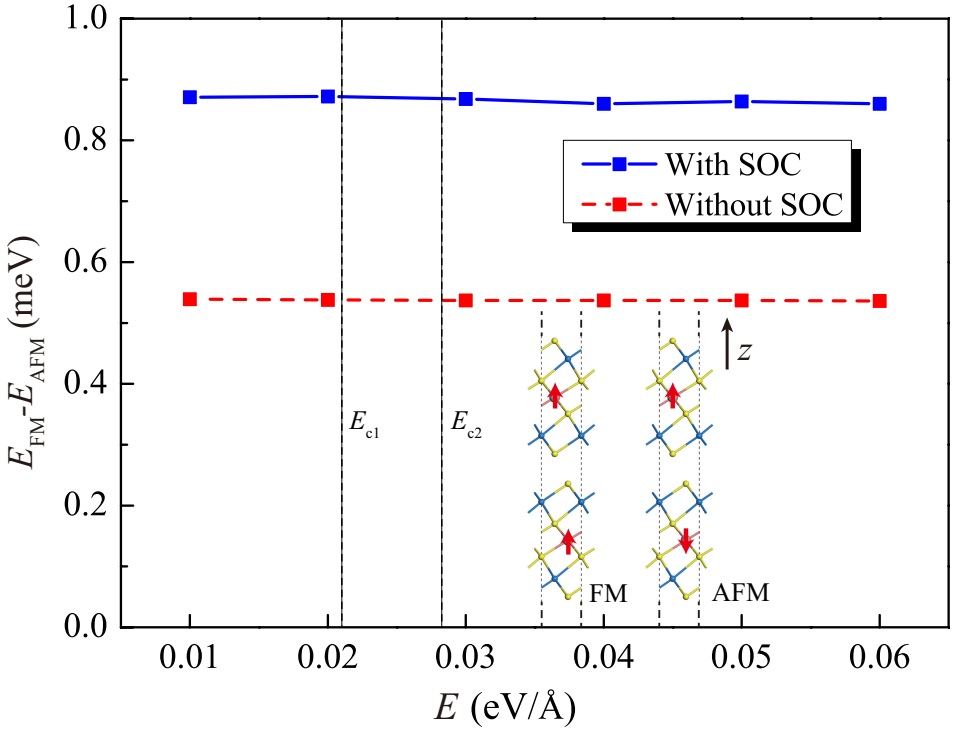

FIG. S2: The magnetic order in double-SL $MnBi_2Te_4$ thin film under electric field. The total energies difference per cell of double-SL $MnBi_2Te_4$ thin films under electric field between the intralayer FM order (E_{FM}) and AFM order (E_{AFM}). The blue and red lines are obtained from DFT calculations with SOC and without SOC, respectively. Insets show the FM and AFM orders in double-SL $MnBi_2Te_4$ thin films. The system keeps AFM order as the ground state under a finite electric field.The black dash lines mark the critical electric field E_{c1} and E_{c2}.

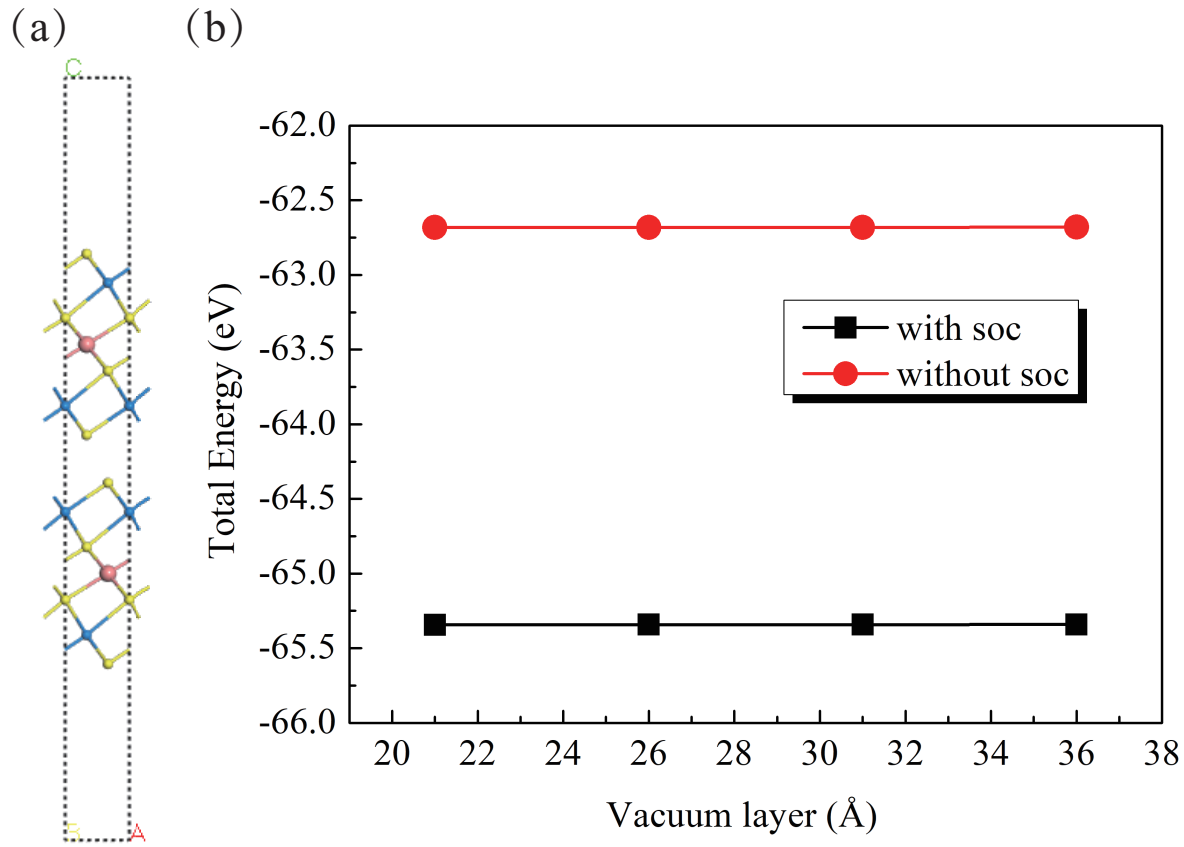

FIG. S3: Convergence test for the thickness of the vacuum layer.(a) The unit cell used in our calculations. (b) The total energies of the double-SL $MnBi_2Te_4$ thin films vary with vacuum layer.

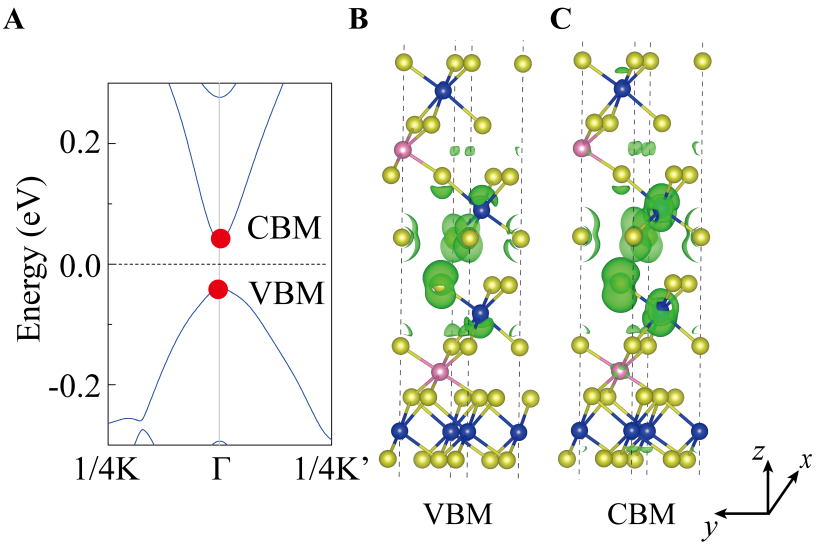

FIG. S4: Partial charge density at band edges of double-SL $MnBi_2Te_4$ thin film. (**A**) Intrinsic band structure of double-SL $MnBi_2Te_4$ thin film. Red solid points mark the doublely degenerate valence band maximum (VBM) and conduction band minimum (CBM). The Fermi level is set to zero. (**B**) Charge density at VBM plotted in green. The isosurface value is 0.0014 eÅ^{-3}. (**C**) Charge density at CBM plotted in green. The isosurface value is 0.001 eÅ^{-3}. The red, blue and yellow balls represent Mn, Bi and Te atoms respectively. As shown in (**B**) and (**C**), VBM is mainly contributed by the out-of-plane orbitals around Te atoms and in-plane orbitals around Bi atoms while the CBM is mainly contributed by the out-of-plane orbitals around Te atoms.

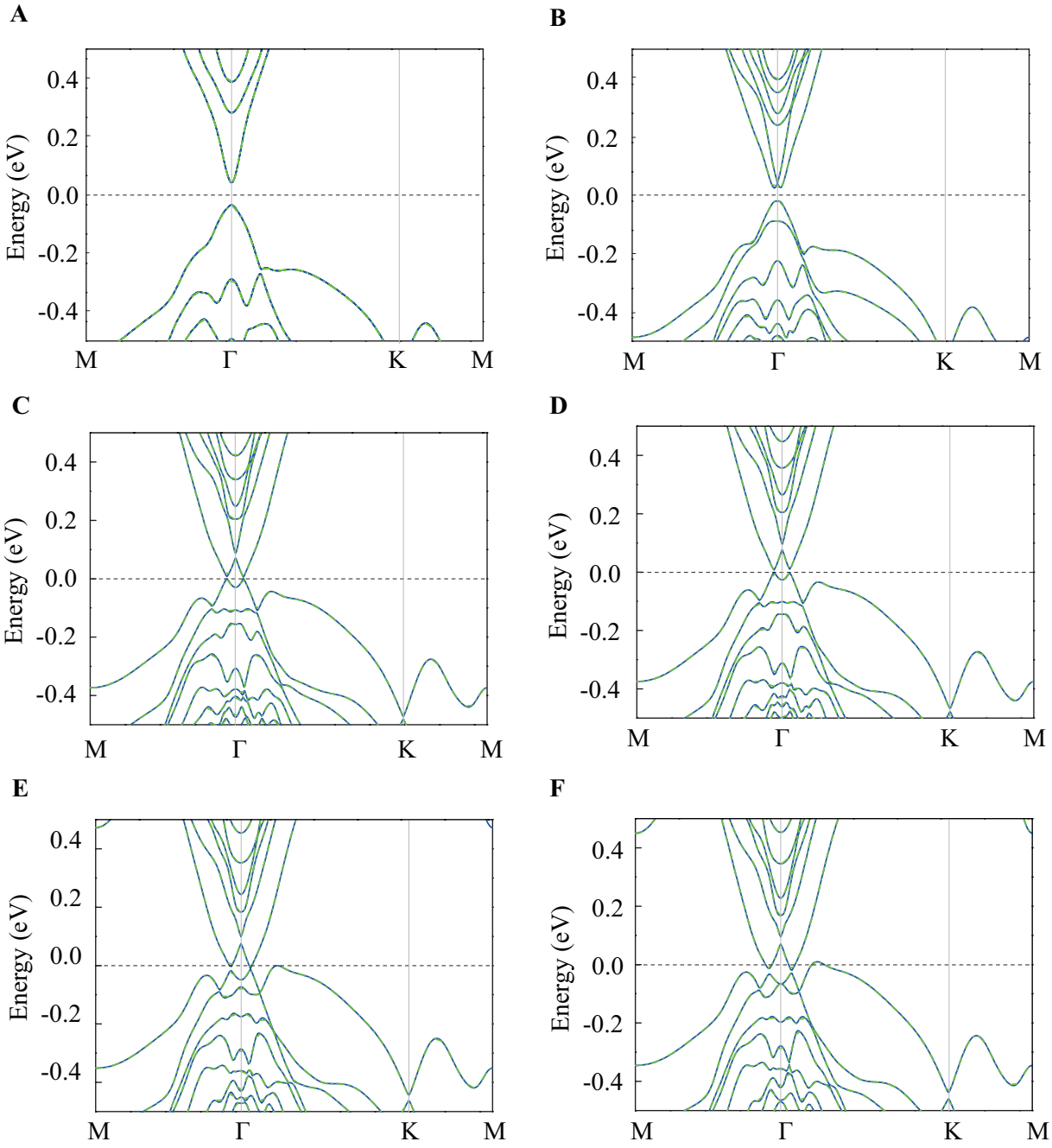

FIG. S5: Wannier interpolated band structures of double-SL $MnBi_2Te_4$ thin film under different electric fields E. Blue solid lines: the band structures from DFT calculations. Green dash lines: the Wannier-interpolated band structures. The Fermi level is set to zero. (**A-F**) The band structures of double-SL $MnBi_2Te_4$ thin film with different electric fields, the magnitudes of electric fields are 0, 0.010, 0.021, 0.023, 0.027, 0.029 V/Å, respectively.

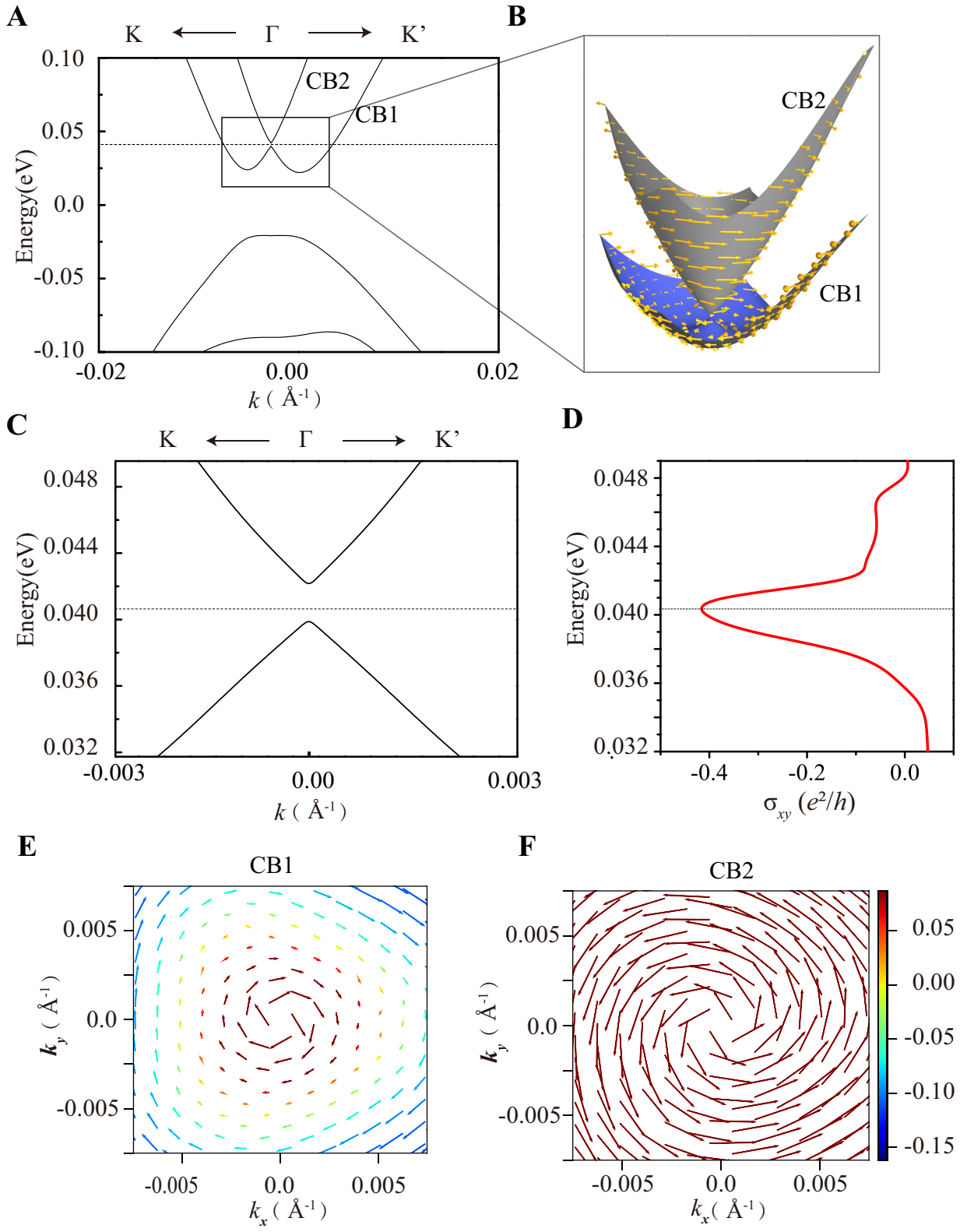

FIG. S6: Spin textures of double-SL $MnBi_2Te_4$ thin film with E=0.010 V/Å. (**A**) Band structure of double-SL $MnBi_2Te_4$ thin film under E= 0.010 V/Å. The energy bands at the anti-crossing point are labeled as CB1 and CB2. (**B**) The spin textures for CB1 and CB2. The yellow arrows indicated the spin polarizations. It is noted that the directions of spin polarization is opposite for CB1 and CB2. (**C**) The electronic bands for CB1 and CB2 around the anti-crossing point. (**D**) AH conductance as a function of chemical potential. The black dashed line shows the energy level that corresponds to the negative AH effect in the Fig. 3b in the main text. (**E-F**) 2D schemes of spin-textures for CB1 and CB2. The arrows represent in-plane spin component whose length stands for the magnitude of corresponding spin polarization, and the color shows out-of-plane spin component. The magnitude of each spin vector is normalized.

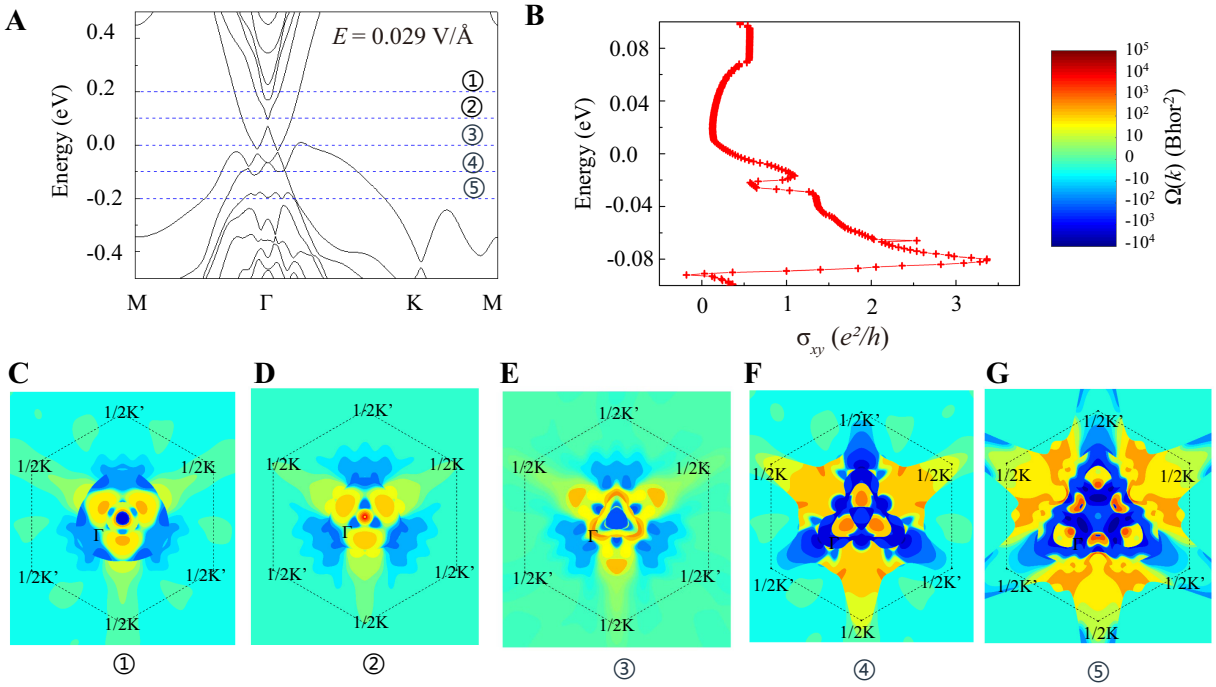

FIG. S7: Berry curvature in the first BZ for double-SL $MnBi_2Te_4$ thin film with E= 0.029 V/Å. (**A**) The band structure when E= 0.029 V/Å. Under such electric field, the double-SL $MnBi_2Te_4$ is a trivial AFM metal. (**B**) AH conductance with as a function of chemical potentials in double-SL $MnBi_2Te_4$ thin film with E= 0.029 V/Å. (**C-G**) The Berry curvature distributions in first BZ at different energy positions as marked in (**A**). It notes that the AH signal increases rapidly as the energy position shifts downwards.

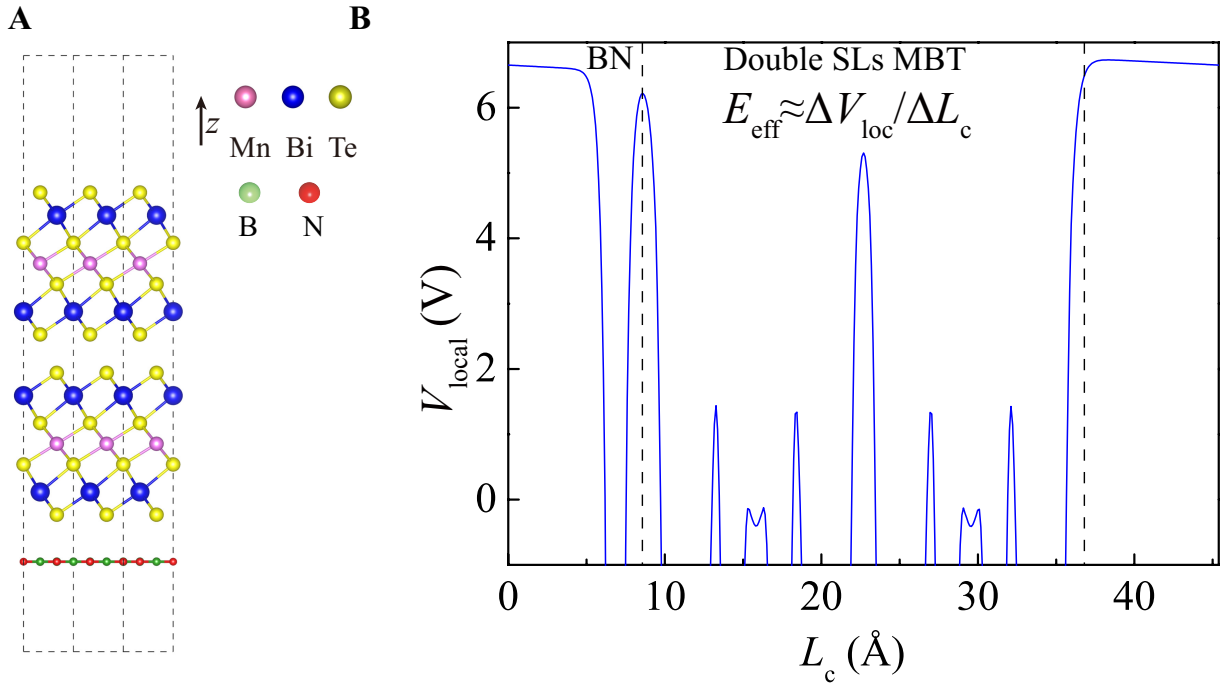

FIG. S8: Effective electric field induced by the substrate. (**A**) Lattice structure of double-SL $MnBi_2Te_4$ thin film on substrate of BN. (**B**) Local potential distribution along the z direction when double-SL $MnBi_2Te_4$ thin film is on the substrate of BN. Black dash lines show the interface between the BN and double-SL $MnBi_2Te_4$ thin film, and the boundary between double-SL $MnBi_2Te_4$ thin film and vacuum region. The potential difference $\Delta V_{\text{loc}} \approx$ 0.46 V, correspondingly, $\Delta L_{\text{c}} \approx 45$ Å, so the effective electric field $E_{\text{eff}} \approx \Delta V_{\text{loc}} / \Delta L_{\text{c}} \approx 0.010$V/Å.

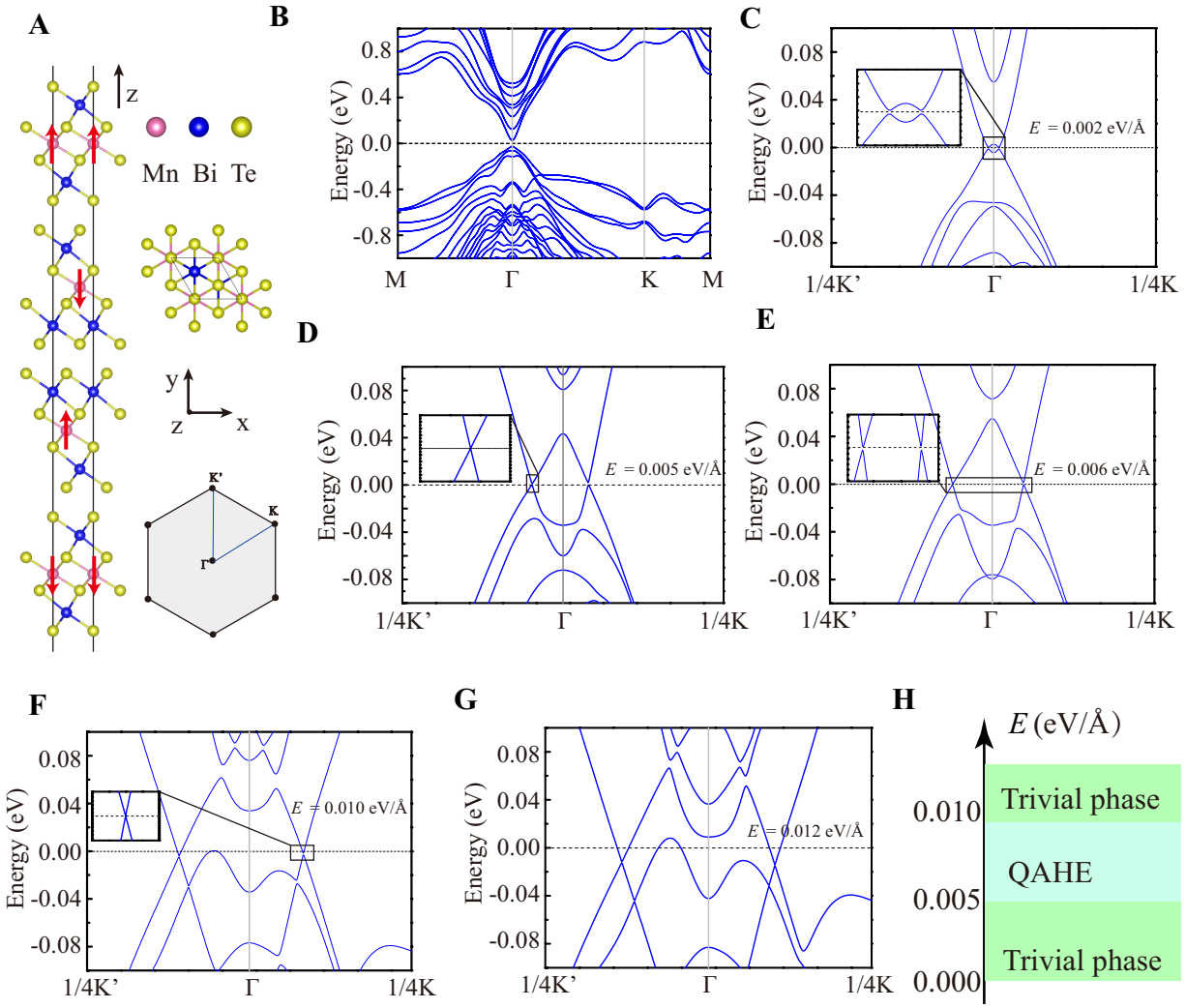

FIG. S9: Band structures and topological phase transitions for four-SL $MnBi_2Te_4$ thin film under electric field (**A**) Lattice structure of four-SL $MnBi_2Te_4$ thin film and its first BZ. (**B**) Intrinsic band structure of four-SL $MnBi_2Te_4$ thin film. (**C-G**) Band structures of four-SL $MnBi_2Te_4$ thin film under different electric fields. From (**C-G**), the magnitudes of electric fields are 0.002, 0.005, 0.006, 0.010, 0.012 V/Å, respectively. The Fermi levels are set to be zero. All of results are calculated from PBE+U with SOC. (**H**) Schematic diagram of topological phase transitions in four-SL $MnBi_2Te_4$ thin film under electric field. The first critical point is E=0.005 V/Å, the band crossing points are on lines of Γ-K', as shown in the inset of (**D**). Correspondingly, the system transforms from a trivial phase to the QAH phase. The second critical point is E=0.010 V/Å, the band crossing points are on lines of Γ-K, as shown in the inset of (**F**). At this time, the system becomes a trivial AFM metal.